

Automated Workflow for Instant Labeling and Real-Time Monitoring of Monoclonal Antibody N-Glycosylation

Aron Gyorgypal^{1,2}, Oscar Potter³, Antash Chaturvedi¹, David N. Powers², Shishir P. S. Chundawat^{1*}

¹Department of Chemical and Biochemical Engineering, Rutgers University, Piscataway, New Jersey, USA

²Center for Drug Evaluation and Research, Office of Product Quality, Office of Biotechnology Products, Division of Biotechnology Review and Research II, U.S. Food and Drug Administration (FDA), Silver Spring, Maryland, USA

³Agilent Technologies, Inc., 5301 Stevens Creek Blvd Santa Clara, California, USA

*Corresponding Author: Shishir P. S. Chundawat (shishir.chundawat@rutgers.edu)

Keywords: Biomanufacturing, process analytical technology, monoclonal antibody, N-glycosylation

Disclaimer: This article reflects the views of the author/s and should not be construed to represent FDA's views or policies.

Abstract

With the transition toward continuous bioprocessing, process analytical technology (PAT) is becoming necessary for rapid and reliable in-process monitoring during biotherapeutics manufacturing. Bioprocess 4.0 is looking to build an end-to-end bioprocesses that includes PAT-enabled real-time process control. This is especially important for drug product quality attributes that can change during bioprocessing, such as protein N-glycosylation, a critical quality attribute for most monoclonal antibody (mAb) therapeutics. Glycosylation of mAbs is known to influence their efficacy as therapeutics and is regulated for a majority of mAb products on the market today. Currently, there is no method to truly measure N-glycosylation using on-line PAT, hence making it impractical to design upstream process control strategies. We recently described the N-GLYcanyzer: an integrated PAT unit that measures mAb N-glycosylation within 3 hours of automated sampling from a bioreactor. Here, we integrated Agilent's Instant PC (IPC) based chemistry workflow into the N-GLYcanyzer PAT unit to allow for nearly 10x faster mAb glycoforms analysis. Our methodology is explained in detail to allow for replication of the PAT workflow as well as present a case study demonstrating use of this PAT to autonomously monitor a mammalian cell perfusion process at the bench-scale to gain increased knowledge of mAb glycosylation dynamics during continuous biomanufacturing of biologics using Chinese Hamster Ovary (CHO) cells.

Introduction

Implementation of advanced PAT and process control in the biopharmaceuticals and bioproducts manufacturing industries continues to lag behind the traditional petrochemical/chemical industry. The current goal towards bioprocess 4.0 is the creation of an end-to-end integrated bioprocess that runs, controls, and continuously improves the process following feed-back/forward control loops enabled by advances in automation and artificial intelligence^{1,2}. However, due to inherent complexities in bioprocesses such as post-translational modifications of therapeutic proteins during biomanufacturing, the creation of PAT tools to continually monitor the critical quality attributes (CQA's) of biologics is a challenge in itself³⁻⁵. A current bottleneck for both bioprocess and bioproduct characterization is the combination of high-throughput and autonomous PAT with high-resolution product quality analytics⁶.

N-linked glycosylation of proteins has garnered attention as a critical quality attribute for many biologic products, especially monoclonal antibodies (mAbs), as macro-heterogeneity in mAb glycoform structures are known to influence the pharmacokinetics, pharmacodynamics, and immunogenicity of

50 the final drug product^{7,8}. N-linked glycosylation is conserved for IgG monoclonal antibodies on their
51 heavy chain at the Asn-297 site, with some products also having N-glycosylation in the variable region as
52 well. The heterogeneity of N-linked glycosylation comes from the multitude of variations in the glycan
53 branches due to the high number of sugar moieties possible as well as the specific linkages present that
54 is influenced by the activity of different glycosidases and glycosyltransferases during cell growth,
55 stationary, and death phases^{8,9}. The glycosylation pattern tends to be also sensitive to the process
56 parameters and the extracellular environment consequently. These parameters are known as critical
57 process parameters (CPPs) and include cell culture temperature, pH, dissolved oxygen concentration,
58 and agitation rate¹⁰⁻¹⁴. Because of this, a process must be well defined to make the glycosylation
59 patterns reproducible between multiple batches¹⁵. Additional complexity is further added if the mAb
60 product of interest is a biosimilar that has stricter tolerances for CQAs to match the originator or
61 innovator drug product^{16,17}.

62
63 Released glycan analysis often involves enzymatic deglycosylation of mAbs isolated from the cell culture
64 using Peptide:N-glycosidase F (PNGase F), followed by glycan labeling by suitable fluorophore tag and
65 labeled glycan enrichment using solid phase extraction (SPE). Traditional methods involve isolated mAb
66 denaturation before a 4-24 hour incubation period for deglycosylation followed by an optional cleanup
67 step to remove deglycosylated protein from the solution. Next, a 2-3 hour incubation step is necessary
68 for fluorescently labeling the released glycan using reductive amination to conjugate a fluorophore like
69 2-aminobenzenamide (2-AB) to the reducing end of the glycans to increase analytical sensitivity. Finally,
70 the excess label is then removed using solid phase extraction (SPE), and the sample is then dried and
71 reconstituted into a suitable matrix before analysis by High-Performance Liquid Chromatography (HPLC)
72 system coupled to a suitable Fluorescence Detector (FLD). This whole process can take anywhere from
73 2-3 days from start to end¹⁸. However, newer technology can allow this workflow to be further
74 streamlined, such as using proprietary PNGase F kits to reduce deglycosylation reaction times to under
75 few minutes, as well as using instant labeling chemistries that allow for nearly instantaneous
76 fluorophore-glycan conjugation. Such technologies can condense the overall N-glycan release and
77 sample prep workflow to less than one hour¹⁹. Examples of such proprietary chemistry kits include
78 Agilent's AdvanceBio Gly-X Technology, as well as Waters' GlycoWorks RapiFluor-MS^{20,21}. While such
79 recent innovations have been able to speed up sample preparation time as well as increase throughput
80 using a 96-well plates design, these kits are not suitable for in-process real-time testing during
81 manufacturing and are more suitable for quality control (QC) based analysis²².

82
83 Here, we look to enable rapid near real-time analysis of mAb N-glycans by integrating the Agilent Gly-X
84 Instant Procainamide (IPC) chemistry and workflow into the N-GLYcanalyzer PAT system. This will allow for
85 faster mAb glycoforms analysis during bioprocessing compared to the traditional 2-AB labeling approach
86 that was recently reported²³. We also show the utility of using the IPC tag to deconvolute glycan peaks
87 using at-line integrated liquid chromatography based mass spectrometry (LC-MS). We demonstrate how
88 instant IPC chemistry can be integrated into an online PAT workflow for automated analysis of mAb
89 glycoforms. Finally, we highlight a case study demonstrating the utility of this automated PAT workflow
90 to rapidly monitor mAb glycoforms produced by a CHO cell perfusion bioprocess.

91 92 **Materials and Methods**

93
94 **Cell line and shake flask cell culture:** The Chinese Hamster Ovary (CHO-K1) cell line producing a
95 recombinant trastuzumab, a biosimilar for Herceptin, was kindly donated by GenScript Biotech
96 Corporation (Piscataway, NJ). A seed train was started by thawing one ampule of cells (10×10^6 cell/mL)
97 from the working seed bank into high intensity perfusion CHO (HIP-CHO) medium (Thermo Fischer

98 Scientific, Waltham, MA) into a 125 mL unbaffled shake flask (VWR, Radnor, PA) with a 40 mL working
99 volume to a seed density of 0.5×10^6 cells/mL containing 0.1% anticlumping agent (Thermo Fischer
100 Scientific, Waltham, MA). The cells were grown at 37°C, 130 RPM, and 8% CO₂ in a New Brunswick S41i
101 CO₂ Incubator (New Brunswick Eppendorf, Hamburg, Germany) for 4 days and passaged twice to 0.5×10^6
102 cell/mL into a 250 mL shake flask and then into a 500 mL shake flask, and then grown for 4 days before
103 inoculation into the bioreactor.

104
105 **Perfusion bioreactor cell culture:** The bioreactor cell culture experiments were conducted in a 3L glass
106 bioreactor using Biostat B-DCU controller (Sartorius, Göttingen, Germany) with a working volume of
107 1.75L. Temperature and pH control was initiated before inoculation and set at 37°C and pH 7.1,
108 respectively. Dissolved oxygen (DO) was also brought to a setpoint of 50% DO. The pH was controlled by
109 sparging either CO₂ or by bolus additions of 0.5M NaOH (Sigma Aldrich, St. Louis, MO). The bioreactor
110 was inoculated to an initial density of 0.5×10^6 cells/mL. Offline samples were taken daily to analyze
111 various culture parameters (e.g., glucose, lactate, glutamate, glutamine, Na, K, Ca) on a BioProfile Flex2
112 Analyzer (Nova Biomedical, Waltham, MA). Product titer was analyzed offline from spent media daily by
113 protein A chromatography on the Agilent Bioinert 1260 HPLC system using a Bio-Monolith Recombinant
114 Protein A column (Agilent Technologies, Santa Clara, CA). An XCell™ ATF system (Repligen, Waltham,
115 MA) was used for steady-state perfusion slowly ramping up the exchange rate from 0.25 to 1.0 vessel
116 volumes a day (VVD) between day 4 and day 8. The bleed rate was also adjusted proportionally with the
117 permeate rate using the pumps to maintain a constant VVD and cell viability throughout the culture
118 duration.

119
120 **Off-line N-glycan sample preparation and analysis:** Offline N-glycan analysis was done using
121 AdvanceBio Gly-X N-glycan prep with InstantPC (GX96-IPC, Agilent Technologies, Santa Clara, CA)
122 following the manufacturer's instructions. Briefly, spent media was removed from the bioreactor daily
123 and the sample was purified using a Protein A HP SpinTrap (Cytiva, Marlborough, MA) with 20mM
124 phosphate buffer pH 7.2 as a binding buffer and 0.1% formic acid as the eluent. The sample was then
125 neutralized using 1M HEPES Solution pH 8.0 to a neutral pH before buffer exchange into 50 mM HEPES
126 solution pH 7.9 and then concentrated to ~2 g/L using a 10 kDa MWCO spin column (VWR, Radnor, PA).
127 Next, 2 µL of Gly-X denaturant was added to 20 µL of the sample prior to heating it to 90°C for three
128 minutes. After cooling, 2 µL of N-Glycanase working solution (1:1 Gly-X N-Glycanase, Gly-X Digest Buffer)
129 was added, mixed, and incubated at 50°C for five minutes. Afterward, 5 µL of Instant PC Dye solution
130 was added, mixed, and incubated for an additional 1 minute at 50°C. The sample was then diluted with
131 150 µL of load/wash solution (2.5% formic acid, 97.5% acetonitrile (ACN)). Next, 400 µL of load/wash
132 solution was added to the Gly-X Cleanup Plate along with the ~ 172 µL of sample. A vacuum was applied
133 (<5 inches Hg) until the sample passed through. Samples were then washed twice with 600 µL of
134 Load/Wash solution before being eluted into a collection plate with 100 µL of Gly-X InstantPC Eluent
135 with vacuum (<2 inches Hg). These samples were run on a 1260 Infinity II Bio-Inert LC System (Agilent
136 Technologies, Santa Clara, CA) using an AdvanceBio Glycan Mapping column 2.1 X 150 mm 2.7 micron
137 (Agilent Technologies, Santa Clara, CA). Mobile phase A was 50 mM ammonium formate adjusted to pH
138 4.4 using formic acid and mobile phase B was acetonitrile. The flow rate was set to 0.5 mL/min, and FLD
139 was set to ex. 285 nm/ em. 345 nm, column temp was at 55°C. The initial eluent was held at 80% B for 2
140 minutes then dropped immediately to 75% B. From 2 minutes to 30 minutes the eluent was changed
141 from 75% B down to 67% B in a linear gradient, and then from 30 to 31 minutes it was decreased from
142 67% B down to 40% B. From 31 to 33.5 minutes the ACN concentration was brought back to 80% at
143 which level it was held until the end of the run at 45 minutes. Relative abundances of individual
144 glycoforms was done on OpenLab CDS v3.5 (Agilent Technologies, Santa Clara, CA).

145

146 **Automated mAb titer analysis using N-GLYcanyzer:** Titer was checked at least once a day using the N-
147 GLYcanyzer system using the ProSIA subunit (FIALab Instruments, Seattle, WA) following the method
148 described in a previous study²³. Briefly, bioreactor supernatant was pumped from the bioreactor
149 through a filtration membrane and sent to the ProSIA system that integrated with a miniature protein A
150 column. The column was machined in-house using PEEK (polyether ether ketone) material with an inner
151 diameter of 2 mm and length of 30 mm and was packed with MabSelect SuRe Protein A resin
152 (MilliporeSigma, Burlington, MA). Once mAb was adsorbed on the column the samples were washed
153 with 20 mM phosphate buffer pH 7.2 and then eluted using 200 μ L of 0.1% formic acid. The eluted
154 sample was sent through an in-line UV spectrometer (Ocean Optics, Dunedin, FL) that was integrated
155 downstream of the Protein A column, measuring at 280 nm wavelength. The integrated peak was used
156 to calculate protein titer against a 7-point calibration curve (MedChemExpress, Monmouth Junction,
157 NJ). If the concentration was found to be sufficient, the sample of purified mAb was then used for
158 released glycan sample preparation (as described below). However, if the concentration was found to be
159 too low for the optimized automated N-GLYcanyzer method analytical range (i.e., less than 100 μ g mAb
160 in eluent), a larger cell-free sample was automatically drawn from the reactor and purified to increase
161 the amount of purified mAb. The sample with desired concentration was then sent to the second sub-
162 unit (N-GLYprep) for further sample preparation of the glycans from mAb.

163

164 **Automated N-glycan preparation and analysis using N-GLYcanyzer:** Scheme 1 depicts the overall
165 workflow (Scheme 1A) and the flow path of the N-GLYcanyzer system (Scheme 1B). After mAb protein
166 purification, glycan analysis was initiated on the N-GLYprep subunit as shown in scheme 1B. The sample
167 was eluted from the Protein A column (having a volume of 200 μ L as described above) and neutralized
168 with 20 μ L of 1M HEPES solution, pH 8. The neutralized sample was then homogenized within the
169 syringe pump and all but 40 μ L was sent to waste. Homogenization was done by aspirating and
170 dispensing the sample to and from the syringe pump through a clear waste line. The remaining 40 μ L
171 homogenized sample was mixed with 4 μ L of Gly-X denaturant, dispensed to the 90°C heated coil for 3
172 minutes, then aspirated back to the syringe pump to allow it to cool to room temperature. For
173 deglycosylation, 4 μ L of a N-Glycanase working solution was aspirated to the sample in the syringe,
174 homogenized, and dispensed to the 50°C heated coil for 5 minutes and then aspirated back into the
175 syringe pump. Labeling was done by aspirating 10 μ L of IPC label to the sample within the syringe and
176 dispensing the sample to the 50°C heater for 1 minute and then aspirating back to the syringe. The
177 sample was then homogenized, and all but 1 μ L was dispensed to waste. The 1 μ L sample was then
178 diluted with 250 μ L of the wash solution (80% acetonitrile, 20% water) by aspirating the wash solution
179 into the syringe and allowing it to mix with the 1 μ L of sample. The wash solution mixed sample was
180 then loaded onto a 2.1 x 5 mm trapping column (821725-906, AdvanceBio Glycan Mapping Guard
181 Column) placed on an external valve (G5631A, 1290 Infinity II Valve Drive, Agilent Technologies, Santa
182 Clara, CA) and washed with another 250 μ L wash solution before the external valve was switched in-line
183 with the analytical HPLC column and the HPLC gradient was started.

184

[Scheme 1]

185

186 Results and Discussion

187

188 **System Automation – Protein A Purification:** The system used a 2 mm x 30 mm length column that was
189 packed with MabSelect SuRe Protein A resin to purify the monoclonal antibody from the extracellular
190 broth of the bioreactor culture. The binding buffer was 20 mM phosphate buffer pH 7.2 and the elution
191 buffer was 0.1% formic acid. The column was conditioned before use. A fixed volume of cell-free reactor
192 culture (200 μ L) was removed using the filtration probe and pumped onto the protein A column. The

193 sample was washed with the binding buffer before elution with 200 μ L of 0.1% formic acid. During this
194 time the eluent is monitored using UV 280 nm absorbance to calculate the mAb titer. If the
195 concentration is too low for subsequent analysis the assay has been automated to be re-run at a higher
196 sampling volume from the reactor to increase the final mAb concentration in the eluent. Afterwards the
197 mAb eluent was neutralized to a pH of 7.9 – 8.0 using 20 μ L of 1M solution of HEPES at pH 8.0. Prior
198 experiments used a Tris-base solution for neutralization; however, it was found that tris-base interfered
199 with the IPC labeling chemistry and was therefore discontinued for the online workflow. A sensitivity
200 study was also run to measure the lowest limit of detection of the assay that are shown in
201 **supplementary figure S1**. Based on the sensitivity study, we found that a mAb concentration as low as
202 0.1 g/L was sufficient for HPLC-FLD analysis, while 0.5 g/L gave better resolution of smaller eluting
203 peaks. From this analysis it was decided that mAb would be concentrated to at least 0.5 g/L prior to
204 glycan preparation post-protein A cleaning.

205
206 [Scheme 2]

207
208 **System automation – deglycosylation and labeling:** The integration of a bench-top assay based on
209 manual steps into a flow-chemistry PAT system is non-trivial. Differences exist between the sample
210 preparation for 2-AB and IPC based labeling chemistry. Labeling with 2-AB depends on a Schiff-base
211 reductive amination of the released N-glycan reducing end moiety (after PNGase F treatment and
212 spontaneous conversion of the glycosylamine product to a sugar aldehyde moiety) with the primary
213 amine functional group of 2-AB forming an imine intermediate before reduction to a stable secondary
214 amine. Conversely, the IPC method relies on a stable urea linkage formation between the instant
215 procainamide label and the glycosylamine product formed immediately after PNGase F cleavage. This
216 glycosylamine is unstable under non-alkaline conditions, losing its primary amine group which is
217 necessary for the urea linkage formation^{24,25}. The reaction schemes are summarized in **scheme 2**
218 showing the PNGase F enzymatic reaction along with the subsequent IPC versus 2-AB based released N-
219 glycan chemical reactions.

220 [Figure 1]

221
222 A study was conducted to measure the labeling efficiency of IPC onto the glycosylamine as a function of
223 PNGase F incubation time at two pH values: pH 7.5 and 8.0. The fluorescence intensity of GOF glycoform
224 released from trastuzumab was monitored to examine the impact of PNGase F incubation time on
225 relative concentration of glycosylamine intermediates release/labeled. This experiment provided some
226 understanding of the relative amounts of glycosylamine intermediates formed after enzymatic cleavage
227 to be readily available for IPC labeling. This provided insight to the optimum reaction time needed as
228 PNGase F cleavage to release increasing concentration of glycosylamine intermediates was impacted by
229 the subsequent hydrolysis of the intermediate to reducing sugars versus intermediate labeling by IPC
230 probe. **Figure 1A** depicts representative chromatograms from the pH 7.5 assay condition. No bias was
231 seen in the relative glycosylation pattern between all sample conditions and replicates for varying
232 incubation times under either pH condition (data not shown). **Figure 1B** shows the integrated
233 fluorescence intensity as arbitrary units (a.u.) of the most abundance labeled glycoform (GOF) as a
234 function of the incubation time and pH. Interestingly, it was seen that in both cases the fluorescent
235 intensity was high after 5 minutes of incubation, 12.94 \pm 0.67 a.u. at pH 7.5 and 12.65 \pm 0.32 a.u. at pH 8.0.
236 The fluorescence intensity dropped at an incubation time of 10 minutes to 2.68 \pm 0.33 a.u. (pH 7.5) and
237 4.29 \pm 2.41 a.u. (pH 8.0). However, the fluorescence value was regained again under the pH 8 condition
238 after 30 minutes to 14.41 \pm 1.42 a.u. and then stayed stable up to 30 minutes. However, under the pH 7.5
239 conditions, the fluorescence value stayed low even up to 30 minutes and then slowly increased to level
240 off only after around 60 minutes to around 8.23 \pm 1.53 a.u. While both conditions started with the same

241 amount of substrate/enzyme (i.e., mAb and PNGase F), the amount of free glycosylamine available for
242 the IPC reaction is almost twice as high at the higher pH reaction condition after one hour of incubation
243 time. This can be attributed to the solution being slightly more alkaline and thus increasing free
244 glycosylamine stability in solution prior to labeling with IPC.

245
246 To the best of our knowledge, there is no open literature that explains the dramatic decrease in free
247 glycosylamine available to dye conjugation between the 5- and 10-minute reaction times. Furthermore,
248 there are many potential unknowns in attempting to explain the mechanism behind this dynamic multi-
249 step reaction kinetics behavior. For example, we still have limited knowledge of; (i) the extent of mAb
250 denaturation that impacts subsequent PNGase F accessibility for glycan cleavage, (ii) the activity of
251 PNGase F under varying pH conditions in the presence of the denaturant, and (iii) enzyme activity over
252 time post initial burst phase as substrate available become rate-limiting. Earlier literature has
253 characterized the kinetics of PNGase F, but not in the context of the glycosylamine formation and its
254 subsequent degradation due to IPC labeling^{26,27}. An additional unknown is the relative degradation rate
255 of the intermediate glycosylamine to free-reducing sugar. Interestingly, there may be alternative chair
256 conformations of the glycosylamine that may be labeled as well²⁰ as shown by Kimzey et al. within their
257 application notes when first reporting on the IPC reagent for glycan labeling. Lastly, it is worth noting
258 that pH does have an effect to the amount of glycosylamine available for IPC labeling, as it is known that
259 the stability of glycosylamines is also pH dependent. While these arguments could explain the dynamic
260 change in IPC labeled glycosylamine intermediate concentrations profile, further exploration was
261 outside of the scope of the current project. In conclusion, to support automation and assay throughput
262 we decided to use the 5-minute total incubation time for the enzymatic deglycosylation and IPC labeling
263 step.

264
265 **HILIC trap column sample enrichment and injection:** After glycans are deglycosylated and labeled with
266 IPC, the samples must be purified to remove any excess label and other contaminants that may be
267 present in solution. The offline, bench-top method uses a proprietary HILIC based material to remove
268 such contaminants. This is done by diluting the labeled glycan samples with 0.1% formic acid in
269 acetonitrile and then passing it through the proprietary HILIC material under vacuum, followed by three
270 wash steps before eluting the bound glycan using a propriety eluent. For an online sample preparation
271 methodology, the exact same steps cannot be easily replicated.

272 [Figure 2]

273
274 This problem was solved by instead introducing a small HILIC guard column to function as a trap column
275 on a 6-port external valve off the HPLC, which acts as an extension to the analytical column upstream.
276 This column functions as an enrichment step after IPC labeling and removes most contaminants without
277 significant loss of all labeled glycans. Most of the labeled sample is sent to waste except for 1 μ L which is
278 diluted 1:250 with 80% acetonitrile and then injected into the trap column. Discarding the bulk of the
279 labeled glycan sample facilitates adjusting the remaining solution to a weak HILIC eluent by addition of
280 the 80% acetonitrile to better adsorb onto the HILIC trapping column. The remaining sample fraction is
281 adequate because the fluorescence sensitivity of IPC labeled glycans is very high. The trapping column is
282 then washed with another 250 μ L of 80% acetonitrile. This six-port valve configuration can be seen in
283 **Figure 2B**. For valve position 1 \rightarrow 6: ports 1 and 4 contain the trapping column with port 5 as the inlet
284 from the N-GLYcanzyer system allowing for the sample and wash solution to pass through to waste on
285 port 6. In this valving position, the HPLC bypasses the trap column through ports 3 and 2. Once the
286 sample is injected into the trap column and washed, the internal setting is switched to position 1 \rightarrow 2 in
287 which the trap column is now in-line with the HPLC mobile phase and the analytical column. At this
288 point, the glycans on the trap column act as the extension of the analytical column and with the start of

289 the mobile phase, the gradient decreases the concentration of the organic phase allowing for
290 chromatography to take place. Surprisingly there was no peak broadening or peak shifting taking place
291 with this online set-up and the chromatography for the online prepared samples ran nearly identically to
292 the offline method prepared samples.

293
294 Next, we investigated the impact of sample injection volume onto the trapping column to understand
295 the trapping efficiency or sample recovery. This was done by varying volumes of labeled glycan samples
296 and diluting them to 250 μL before injection on to the N-GLYcanzyer unit. A sample of mAb around ~ 1
297 g/L was used for this experiment. The same sample was used for each injection to minimize batch-to-
298 batch variability. Adjusting the injection volume and wash volume was also done to optimize this step,
299 with 250 μL found to give the best cleaning efficiency versus glycan recovery (data not shown). **Figure**
300 **2B** shows the increase in fluorescence signal with the increase in prepared sample mass and is
301 quantified for three of the most abundant glycoforms in **Figure 2C**. A linear response can be seen with
302 the increase in sample mass up to 16 μL of loaded sample ($r=0.99^2$), with linearity lost after 16 μL . This is
303 quantified in terms of integrated fluorescence values as well as relative abundances in **Table 1A** and **1B**.
304 There was no bias seen in the trastuzumab glycoform patterns upto 16 μL equivalent mass of sample
305 injected onto the column. At the highest sample loading, there was a slight loss in linearity and the
306 glycan distribution showed a decrease in relative abundances for the smaller glycoforms and a
307 proportional increase for the larger glycoforms. For example, the relative abundance of G0F fell from
308 $48.8\% \pm 0.1\%$ to $42.6\% \pm 0.2\%$, and G1F and G1F' went from $27.5 \pm 0.1\%$ and $9.9\% \pm 0.0\%$, respectively
309 to $32.1\% \pm 0.3\%$ and $11.7\% \pm 0.2\%$ relative abundances, respectively. This loss in retention and increase
310 in recovery bias was expected for the highest loadings of samples tested. While increasing the sample
311 loading volume (volume of sample in mostly aqueous buffer) the proportionality of the organic phase
312 (acetonitrile concentration) will decrease leading to weaker retention of smaller glycoforms.
313 Subsequently, larger glycans will tend to have stronger adsorption to the stationary phase causing a bias
314 in sample recovery. Due to these results, we suspect that the trapping column was not overloaded at
315 even the higher injection volumes/masses, but instead it is more likely that the weaker mobile phase
316 caused bias in glycan retention^{28,29}.

317
318 **Figure 3D** show the monoisotopic masses for each trastuzumab glycoform tagged with IPC and analyzed
319 by LC-MS. While IPC is a fluorophore it also contains a tertiary amine which facilitates IPC labeled species
320 ionization in positive mode electrospray ionization mass spectrometry (ESI-MS). The utility of the IPC tag
321 for MS analysis is showcased here to facilitate the concept of using this system with an LC-MS to allow
322 for unknown labeled glycan mass identification. Samples of trastuzumab were analyzed on an offline LC-
323 MS using a slightly longer gradient to allow for increased chromatographic separation prior to MS
324 detection. The LC system was identical as before while the MS system was an Agilent Ultivo Triple
325 Quadrupole mass spectrometer that is compatible with the overall N-GLYcanzyer workflow.

326
327 A similar workflow was proposed by Bénet et al. as an online methodology to clean 2-AB using a trap
328 column³⁰. This workflow injected an impure 2-AB labeled glycan reaction mixture onto an HPLC and
329 trapped the glycans on a BEH amide packed trap column using a 75% acetonitrile isostatic flow for a
330 fixed amount of time to wash the trap column of contaminants while retaining the oligosaccharides
331 before changing the valve position in line with the analytical column. This valve position change
332 reversed the flow on the trap column as it eluted onto the analytical column. However, in our design, we
333 did not change the flow on the trap column. The previous online clean-up workflow was comparable
334 with offline cleaning to remove excess 2-AB as well. Our work shows a similar approach can be adopted
335 using IPC tag over the 2-AB tag while using a superficially porous HILIC trap column.

336

337 Ultimately, it was found that a large volume of glycan sample can be loaded onto the trapping column
338 without causing bias during downstream analytical chromatography step for LC-FLD or LC-MS. The assay
339 was optimized so that around 2 μL of prepared labeled glycan sample will need to be diluted to 250 μL
340 for the final online assay. This volume was chosen based on an analytical sensitivity criteria in case there
341 is any loss in syringe aspiration and dispensation tolerances used during the bioprocess campaign. An
342 increase in the sample volume (pre-dilution) would need only be considered if fluorescent response was
343 found to be low, depending on the mAb glycoform relative composition.
344

345 **Perfusion-based cell culture mAb glycoforms analysis:** To showcase the utility of the N-GLYcanalyzer
346 system integrated with the IPC chemistry workflow, we studied a perfusion bioprocess producing a
347 trastuzumab biosimilar. Perfusion mode of operation can become challenging to measure glycoforms
348 since the mAb titers are considerably lower than that of a fed-batch counterpart as the product is
349 constantly being harvested and cells are being bled to maintain a pseudo-steady state. Titer was
350 measured every day starting at day 0, with glycoform analysis only started once a detectable
351 concentration of mAb was seen in the culture on day 4. Culture harvesting was also started on day 4 at a
352 0.25 VVD, and cell bleeding started around day 6 as the viable cell density approached 20 million
353 cells/mL. At this point, the perfusion rate was changed to 1.0 VVD with the bleed, and harvests were
354 changed proportionally to maintain a semi-constant cell density throughout the 20-day culture.
355

356 **Figure 3A** shows the viable cell density and viability over the 20-day cell culture period. The viability
357 stayed above 90% throughout the culture run and viable cell density maintained roughly between 18
358 and 23 million cells/mL. **Figure 3B** shows the titer monitored within the reactor throughout the culture
359 using the online N-GLYcanalyzer system as well as the standard offline analysis method. The
360 measurements were taken once a day until day 4 and then roughly every 8 hours using the N-
361 GLYcanalyzer system. The offline measurements were done by taking at least two technical replicates
362 ($n=2$), and the online measurements were done once per analysis. The titers measured under both
363 systems showed very similar trends, with the offline measurements giving a slightly higher
364 concentration. Once at a steady state the mAb space-time yield (STY) remained between 0.08 and 0.12
365 g/L/day through the culture.
366

367 The glycan indices (GI) calculated based on all detected trastuzumab glycoforms are shown in **Figure 3C**
368 and **Figure 3D**. The relative galactosylation index was measured and calculated by the summation of all
369 galactosylated glycoforms divided by the summation of all glycoforms, giving the relative level of mAb
370 glycoforms galactosylation within the reactor. The results follow a similar trend as seen in our recent
371 publication²³ where the galactosylation rate tends to be high through the first few days of production
372 (i.e., ~38% rel. galactosylation) and then sharply declines once the cells reach a pseudo-stationary phase
373 (e.g., ~24% rel. galactosylation). The relative galactosylation rate is still within the quality tolerances set
374 by the FDA based on a public release filing for a trastuzumab biosimilar³¹. The relative afucosylation
375 index increased over time from around 4% to 5.5% at the end of the culture. This afucosylation index
376 would be technically out of specification for a US-trastuzumab biosimilar based on a filing for another
377 trastuzumab biosimilar as referenced above.
378

379 Madabhushi et al. proposed that the declining levels of relative mAb galactosylation are caused by an
380 increase in the cellular productivity of mAb that results in decreased residence time within the Golgi
381 apparatus and hence incomplete addition of terminal sugars like galactose to the N-glycan backbone³².
382 Using the N-GLYcanalyzer PAT system, it will be possible in the future to understand the dynamic changes
383 in mAb N-glycosylation more frequently to better quantify the rates of change over time, and develop
384 novel process control strategies to achieve bespoke mAb glycoform profiles. Incorporating a similar PAT

385 system with an advanced multi-omics approach can also help reveal subtle changes within cellular
386 pathways to gain a fundamental understanding of the metabolic bottlenecks impacting protein
387 glycosylation.

388 389 **Conclusion**

390
391 In this study, we have integrated a commercially available N-glycan release/labeling kit chemistry into
392 the N-GLYcanzyer flow chemistry PAT system. This proof of concept system allows for real-time
393 monitoring of a bioprocess to monitor protein N-glycosylation which could allow for future
394 implementation of advanced control strategies during industrial-scale biologic biomanufacturing. The
395 chemistry of glycosylamine formation during the enzymatic deglycosylation step was studied to
396 understand how the relative formation and degradation rates over time at varying pH's impact analytical
397 sensitivity. A trapping column was introduced to the PAT flow system to allow for more accurate IPC
398 labeled glycan capture, enrichment, and injection into a U/HPLC analytical column for fluorescence or
399 mass spectrometric based product detection. The trap column was also characterized by exploring the
400 sample matrix impact on glycan trapping. Lastly, we used the N-GLYcanzyer for automated real-time
401 glycan analysis during a bench scale perfusion bioprocess to demonstrate the utility of the PAT system
402 to measure changes in mAb glycosylation over time, especially monitoring the relative changes in
403 galactosylation and afucosylation indices, two metrics that influence an antibody's pharmacodynamics
404 and pharmacokinetics. The N-GLYcanzyer PAT system will allow for developing a fundamental
405 understanding of the intra/extra-cellular pathways impacting protein glycosylation dynamic flux during
406 both fed-batch and perfusion bioprocessing. Further, such a PAT will allow the development of
407 advanced process control strategies that can autonomously adapt to undesirable process perturbations,
408 such as pH and temperature shifts, as well as desirable perturbations, such as the addition of specific
409 nutrients and media modulators (e.g., sugars, cofactors), that affect the glycosylation pathway to impact
410 drug quality.

411 412 413 **Author contributions:**

414
415 *Aron Gyorgypal*: Conceptualization, Investigation, Methodology, Validation, System Set-up, Formal
416 Analysis, Writing – Original draft, Writing: review & editing. *Oscar Potter*: Investigation, Methodology,
417 Conceptualization, Supervision, Writing – review & editing. *Antash Chaturvedi*: Investigation, Writing –
418 review & editing. *David N. Powers*: Investigation, System Set-up, Validation, Writing – review & editing.
419 *Shishir P.S. Chundawat*: Conceptualization, Investigation, Supervision, Writing – review & editing

420 421 422 **Acknowledgments:**

423
424 This work was supported by the U.S. Food and Drug Administration (FDA) through the FDA-CBER Award
425 1R01FD006588, Agilent Technologies University Relations Grant 4481, PC5.2-112 NIIMBL Project Award,
426 as well as supported in part by the appointment of Aron Gyorgypal to the Research Participation
427 Program at FDA, administered by ORAU through the U.S. Department of Energy Oak Ridge Institute for
428 Science and Education (ORISE). The authors would like to thank Agilent Technologies Inc. (Mr. Wayne
429 Heacock, and Dr. Ace Galermo) for their extensive and timely support of this project. As well as the
430 Office of Biotechnology Products (OBP) Bioprocessing Lab (Dr. Cyrus Agarabi, Dr. Erica Fratz-Berilla, Mrs.
431 Casey Kohnhorst) at the U.S. FDA Center for Drug Evaluation and Research (CDER) for their support in

432 this project. The authors also thank GenScript Biotech Corporation (Piscataway, NJ) for the Trastuzumab
433 cell line gift to Rutgers University.
434
435

436 **References**

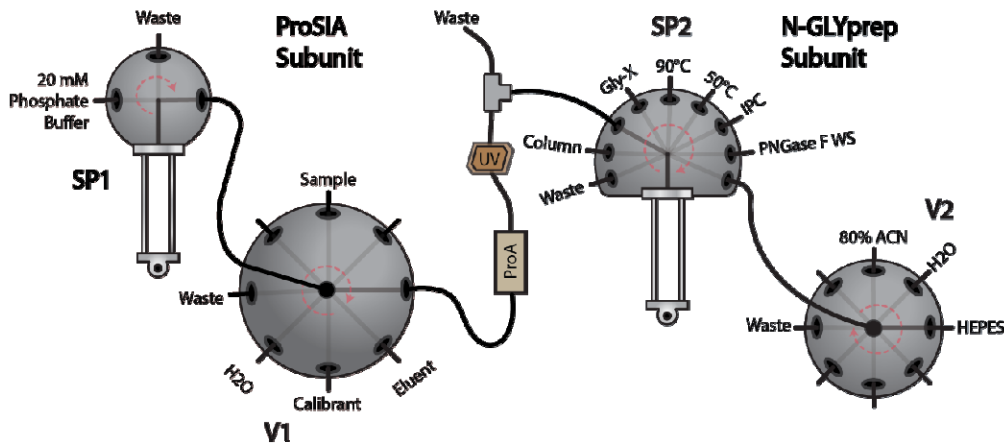
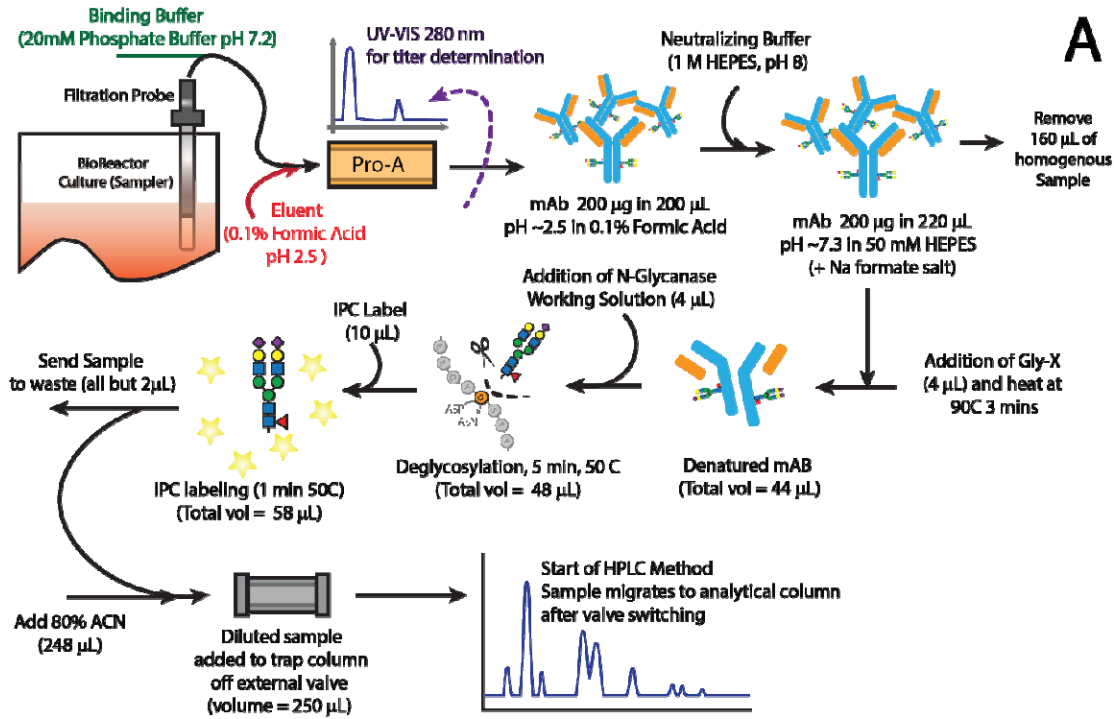
- 437 (1) Gargalo, C. L.; de las Heras, S. C.; Jones, M. N.; Udugama, I.; Mansouri, S. S.; Krühne, U.; Gernaey,
438 K. V. Towards the Development of Digital Twins for the Bio-Manufacturing Industry. In *Advances*
439 *in Biochemical Engineering/Biotechnology*; Springer Berlin Heidelberg: Berlin, Heidelberg, 2020;
440 pp 1–34. https://doi.org/10.1007/10_2020_142.
- 441 (2) Coffman, J.; Brower, M.; Connell-Crowley, L.; Deldari, S.; Farid, S. S.; Horowski, B.; Patil, U.;
442 Pollard, D.; Qadan, M.; Rose, S.; Schaefer, E.; Shultz, J. A Common Framework for Integrated and
443 Continuous Biomanufacturing. *Biotechnol. Bioeng.* **2021**, *118* (4), 1735–1749.
444 <https://doi.org/10.1002/bit.27690>.
- 445 (3) Chopda, V.; Gyorgypal, A.; Yang, O.; Singh, R.; Ramachandran, R.; Zhang, H.; Tsilomelekis, G.;
446 Chundawat, S. P. S.; Ierapetritou, M. G. Recent Advances in Integrated Process Analytical
447 Techniques, Modeling, and Control Strategies to Enable Continuous Biomanufacturing of
448 Monoclonal Antibodies. *J. Chem. Technol. Biotechnol.* **2022**, *97* (9), 2317–2335.
449 <https://doi.org/10.1002/jctb.6765>.
- 450 (4) Stolfa, G.; Smonskey, M. T.; Boniface, R.; Hachmann, A. B.; Gulde, P.; Joshi, A. D.; Pierce, A. P.;
451 Jacobia, S. J.; Campbell, A. CHO-Omics Review: The Impact of Current and Emerging Technologies
452 on Chinese Hamster Ovary Based Bioproduction. *Biotechnol. J.* **2018**, *13* (3), 1–14.
453 <https://doi.org/10.1002/biot.201700227>.
- 454 (5) Kotidis, P.; Kontoravdi, C. Harnessing the Potential of Artificial Neural Networks for Predicting
455 Protein Glycosylation. *Metab. Eng. Commun.* **2020**, *10* (May), e00131.
456 <https://doi.org/10.1016/j.mec.2020.e00131>.
- 457 (6) Konstantinidis, S.; Kong, S.; Titchener-Hooker, N. Identifying Analytics for High Throughput
458 Bioprocess Development Studies. *Biotechnol. Bioeng.* **2013**, *110* (7), 1924–1935.
459 <https://doi.org/10.1002/bit.24850>.
- 460 (7) Higel, F.; Seidl, A.; Sörgel, F.; Friess, W. N-Glycosylation Heterogeneity and the Influence on
461 Structure, Function and Pharmacokinetics of Monoclonal Antibodies and Fc Fusion Proteins. *Eur.*
462 *J. Pharm. Biopharm.* **2016**, *100*, 94–100. <https://doi.org/10.1016/j.ejpb.2016.01.005>.
- 463 (8) Boune, S.; Hu, P.; Epstein, A. L.; Khawli, L. A. Principles of N-Linked Glycosylation Variations of
464 IgG-Based Therapeutics: Pharmacokinetic and Functional Considerations. *Antibodies* **2020**, *9* (2),
465 22. <https://doi.org/10.3390/antib9020022>.
- 466 (9) Butters, T. D. Control in the N-Linked Glycoprotein Biosynthesis Pathway. *Chem. Biol.* **2002**, *9*
467 (12), 1266–1268. [https://doi.org/10.1016/S1074-5521\(02\)00290-9](https://doi.org/10.1016/S1074-5521(02)00290-9).
- 468 (10) Yang, O.; Ierapetritou, M. Mab Production Modeling and Design Space Evaluation Including
469 Glycosylation Process. *Processes* **2021**, *9* (2), 1–19. <https://doi.org/10.3390/pr9020324>.
- 470 (11) Ivarsson, M.; Villiger, T. K.; Morbidelli, M.; Soos, M. Evaluating the Impact of Cell Culture Process
471 Parameters on Monoclonal Antibody N-Glycosylation. *J. Biotechnol.* **2014**, *188*, 88–96.
472 <https://doi.org/10.1016/j.jbiotec.2014.08.026>.
- 473 (12) Sou, S. N.; Sellick, C.; Lee, K.; Mason, A.; Kyriakopoulos, S.; Polizzi, K. M.; Kontoravdi, C. How Does
474 Mild Hypothermia Affect Monoclonal Antibody Glycosylation? *Biotechnol. Bioeng.* **2015**, *112* (6),
475 1165–1176. <https://doi.org/10.1002/bit.25524>.
- 476 (13) Brunner, M.; Fricke, J.; Kroll, P.; Herwig, C. Investigation of the Interactions of Critical Scale-up
477 Parameters (PH, PO₂ and PCO₂) on CHO Batch Performance and Critical Quality Attributes.
478 *Bioprocess Biosyst. Eng.* **2017**, *40* (2), 251–263. <https://doi.org/10.1007/s00449-016-1693-7>.
- 479 (14) Alhuthali, S.; Kotidis, P.; Kontoravdi, C. Osmolality Effects on CHO Cell Growth , Cell Volume ,
480 Antibody Productivity and Glycosylation. **2021**.
- 481 (15) Goswami, S.; Wang, W.; Arakawa, T.; Ohtake, S. Developments and Challenges for MAb-Based
482 Therapeutics. *Antibodies* **2013**, *2* (4), 452–500. <https://doi.org/10.3390/antib2030452>.
- 483 (16) Duivelshof, B. L.; Jiskoot, W.; Beck, A.; Veuthey, J. L.; Guillaume, D.; D’Atri, V. Glycosylation of

- 484 Biosimilars: Recent Advances in Analytical Characterization and Clinical Implications. *Anal. Chim.*
485 *Acta* **2019**, *1089*, 1–18. <https://doi.org/10.1016/j.aca.2019.08.044>.
- 486 (17) Rathore, A. S.; Chhabra, H.; Bhargava, A. Approval of Biosimilars: A Review of Unsuccessful
487 Regulatory Filings. *Expert Opin. Biol. Ther.* **2021**, *21* (1), 19–28.
488 <https://doi.org/10.1080/14712598.2020.1793954>.
- 489 (18) France, R. R.; Cumpstey, I.; Butters, T. D.; Fairbanks, A. J.; Wormald, M. R. Fluorescence Labelling
490 of Carbohydrates with 2-Aminobenzamide (2AB). *Tetrahedron: Asymmetry* **2000**, *11* (24), 4985–
491 4994. [https://doi.org/10.1016/S0957-4166\(00\)00477-8](https://doi.org/10.1016/S0957-4166(00)00477-8).
- 492 (19) Tiwold, E.; Gyorgypal, A.; Chundawat, S. Recent Advances in Biologic Therapeutic N-Glycan
493 Preparation Techniques and Analytical Methods for Facilitating Biomanufacturing Automation.
494 *ChemRxiv* **2022**.
- 495 (20) Kimzey, M.; Szabo, Z.; Sharma, V.; Gyenes, A.; Tep, S.; Taylor, A.; Jones, A.; Hyche, J.; Haxo, T.;
496 Vlasenko, S. Development of an Instant Glycan Labeling Dye for High Throughput Analysis by
497 Mass Spectrometry. *ProZyme* **2015**, *25*, 1295–1295.
- 498 (21) Lauber, M. A.; Yu, Y.-Q.; Brousmiche, D. W.; Hua, Z.; Koza, S. M.; Magnelli, P.; Guthrie, E.; Taron,
499 C. H.; Fountain, K. J. Rapid Preparation of Released N -Glycans for HILIC Analysis Using a Labeling
500 Reagent That Facilitates Sensitive Fluorescence and ESI-MS Detection. *Anal. Chem.* **2015**, *87* (10),
501 5401–5409. <https://doi.org/10.1021/acs.analchem.5b00758>.
- 502 (22) Kinoshita, M.; Yamada, K. Recent Advances and Trends in Sample Preparation and Chemical
503 Modification for Glycan Analysis. *J. Pharm. Biomed. Anal.* **2022**, *207*, 114424.
504 <https://doi.org/10.1016/j.jpba.2021.114424>.
- 505 (23) Gyorgypal, A.; Chundawat, S. P. S. Integrated Process Analytical Platform for Automated
506 Monitoring of Monoclonal Antibody N-Linked Glycosylation. *Anal. Chem.* **2022**, *94* (19), 6986–
507 6995. <https://doi.org/10.1021/acs.analchem.1c05396>.
- 508 (24) Isbell, H. S.; Frush, H. L. EFFECT OF PH IN THE MUTAROTATION AND HYDROLYSIS OF
509 GLYCOSYLAMINES. *J. Am. Chem. Soc.* **1950**, *72* (2), 1043–1044.
510 <https://doi.org/10.1021/ja01158a527>.
- 511 (25) Isbell, H. S.; Frush, H. L. Mutarotation, Hydrolysis, and Rearrangement Reactions of
512 Glycosylamines. *J. Org. Chem.* **1958**, *23* (9), 1309–1319. <https://doi.org/10.1021/jo01103a019>.
- 513 (26) Du, J. J.; Klontz, E. H.; Guerin, M. E.; Trastoy, B.; Sundberg, E. J. Structural Insights into the
514 Mechanisms and Specificities of IgG-Active Endoglycosidases. *Glycobiology* **2020**, *30* (4), 268–
515 279. <https://doi.org/10.1093/GLYCOB/CWZ042>.
- 516 (27) Bodnar, J.; Szekrenyes, A.; Szigeti, M.; Jarvas, G.; Krenkova, J.; Foret, F.; Guttman, A. Enzymatic
517 Removal of N-Glycans by PNGase F Coated Magnetic Microparticles. *Electrophoresis* **2016**, *37*
518 (10), 1264–1269. <https://doi.org/10.1002/elps.201500575>.
- 519 (28) Qing, G.; Yan, J.; He, X.; Li, X.; Liang, X. Recent Advances in Hydrophilic Interaction Liquid
520 Interaction Chromatography Materials for Glycopeptide Enrichment and Glycan Separation. *TrAC*
521 *Trends Anal. Chem.* **2020**, *124*, 115570. <https://doi.org/10.1016/j.trac.2019.06.020>.
- 522 (29) Qiao, L.; Shi, X.; Xu, G. Recent Advances in Development and Characterization of Stationary
523 Phases for Hydrophilic Interaction Chromatography. *TrAC Trends Anal. Chem.* **2016**, *81*, 23–33.
524 <https://doi.org/10.1016/j.trac.2016.03.021>.
- 525 (30) Bénet, T.; Austin, S. On-Line Cleanup for 2-Aminobenzamide-Labeled Oligosaccharides. *Anal.*
526 *Biochem.* **2011**, *414* (1), 166–168. <https://doi.org/10.1016/j.ab.2011.03.002>.
- 527 (31) Mylan. *FDA Oncologic Drugs Advisory Committee Meeting - MYL-14010 (Mylan's Proposed*
528 *Biosimilar to Trastuzumab)*; **2017**.
- 529 (32) Madabhushi, S. R.; Podtelezhnikov, A. A.; Murgolo, N.; Xu, S.; Lin, H. Understanding the Effect of
530 Increased Cell Specific Productivity on Galactosylation of Monoclonal Antibodies Produced Using
531 Chinese Hamster Ovary Cells. *J. Biotechnol.* **2021**, *329* (February), 92–103.

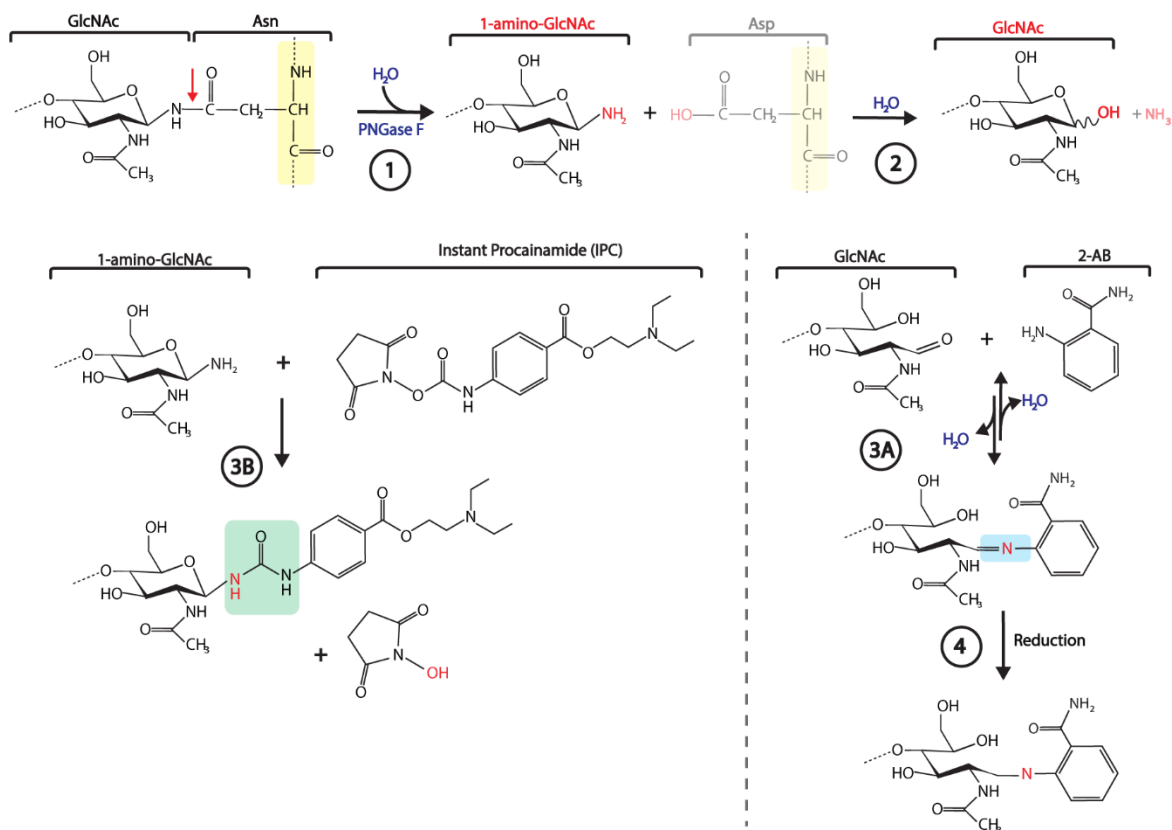
532
533

<https://doi.org/10.1016/j.jbiotec.2021.01.023>.

534 Scheme:
535

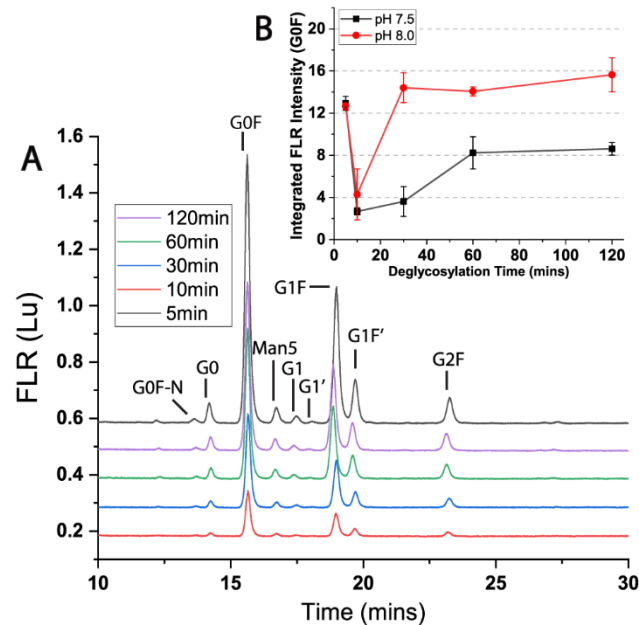


536
537 **Scheme 1: Instant PC glycan labeling chemistry workflow integration with N-GLYcanizer PAT system.** (1A)
538 illustrates sample preparation process outlined within the methods section while (1B) shows the flow paths for
539 sample preparation including syringe pumps 1 and 2 (SP1 and SP2, respectively) as well as the two associated
540 valves (V1 and V2, respectively) within the overall workflow. The colors indicate different subunits: red indicates
541 ProSIA system while blue indicates the N-GLYprep subunit, and gray is found in between the two subunits.
542

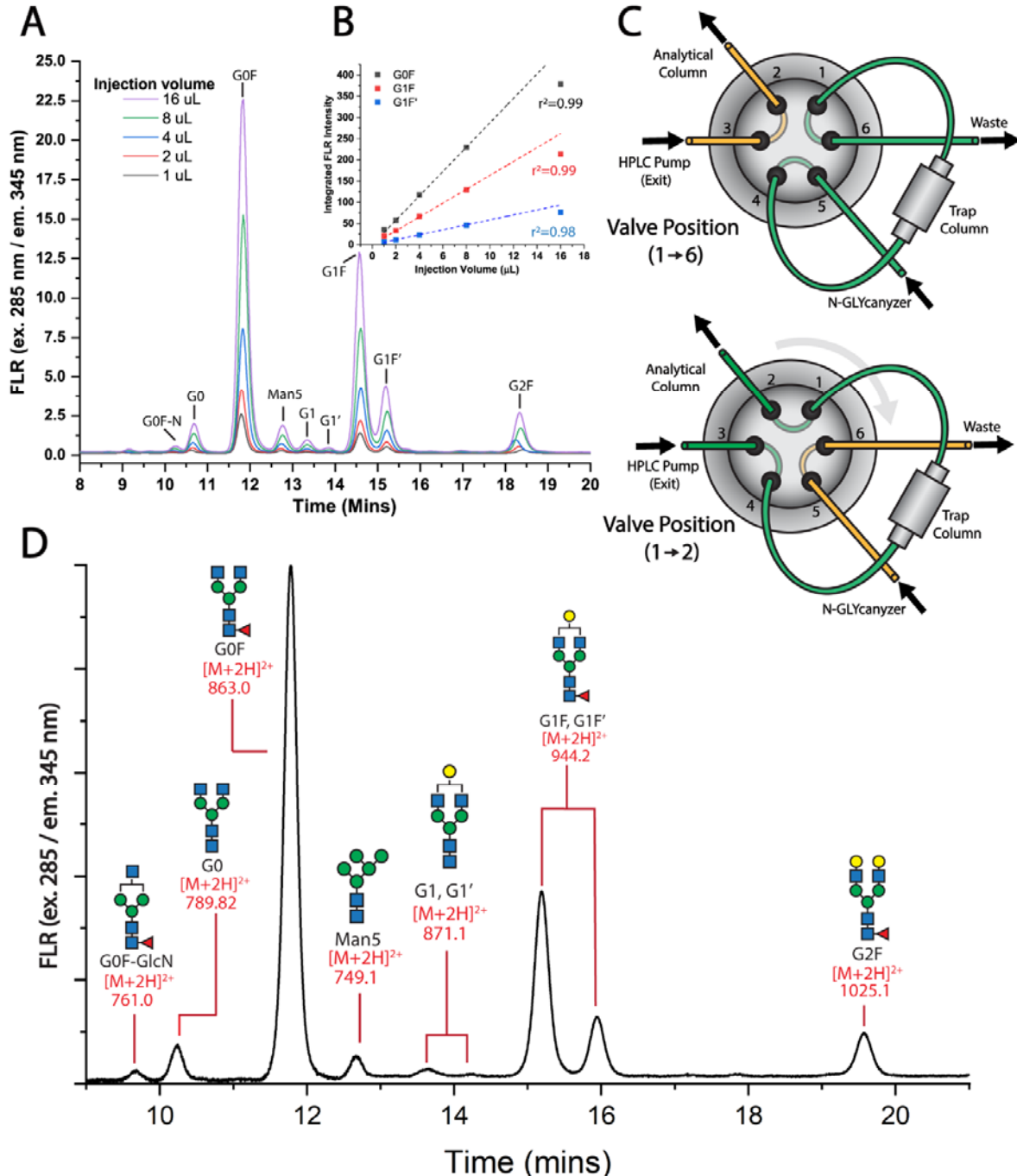


543
 544 **Scheme 2: Reaction scheme associated with the enzymatic deglycosylation reaction followed by labeling**
 545 **chemistries using IPC versus 2-AB is shown here.** In Step (1) the denatured antibody is treated with PNGase F that
 546 cleaves the innermost N-acetylglucosamine (GlcNAc) of the N-glycan from the amino-acid backbone attached via
 547 the asparagine residue. This reaction releases the N-glycan oligosaccharide from the antibody protein backbone
 548 leaving a glycosylamine (1-amino-GlcNAc) intermediate while converting the Asn residue to an aspartate (Asp)
 549 residue. The deglycosylated antibody is no longer needed for the subsequent reactions and is shown as faded in
 550 the reaction scheme. In Step (2) the reaction of the glycosylamine intermediate under slightly non-alkaline
 551 condition and prolonged reaction time in presence of water will lead to loss of an ammonia group that leaves
 552 behind the reducing sugar GlcNAc intermediate. This free reducing sugar can be used as substrate for subsequent
 553 reductive amination reaction. In Step (3A) in the presence of a reactive amine such as 2-AB (a fluorophore) under
 554 high temperature and acidic reaction conditions the reducing sugar moiety of the N-glycan can react to form an
 555 imine intermediate (as shown highlighted in blue), which is unstable in water. In Step (4) the imine intermediate
 556 can be converted to a stable secondary amine in the presence of a strong reducing agent, and this final product is a
 557 N-glycan that is tagged with a 2-AB fluorophore. (3B) Conversely, the glycosylamine intermediate can
 558 instantaneously react with IPC to form a urea linkage (highlighted in green) under moderate reaction conditions
 559 leaving behind an N-Hydroxysuccinimide (NHS) by-product. Here the final product is a N-glycan that is tagged with
 560 a IPC fluorophore group.
 561

562 Figures:
563



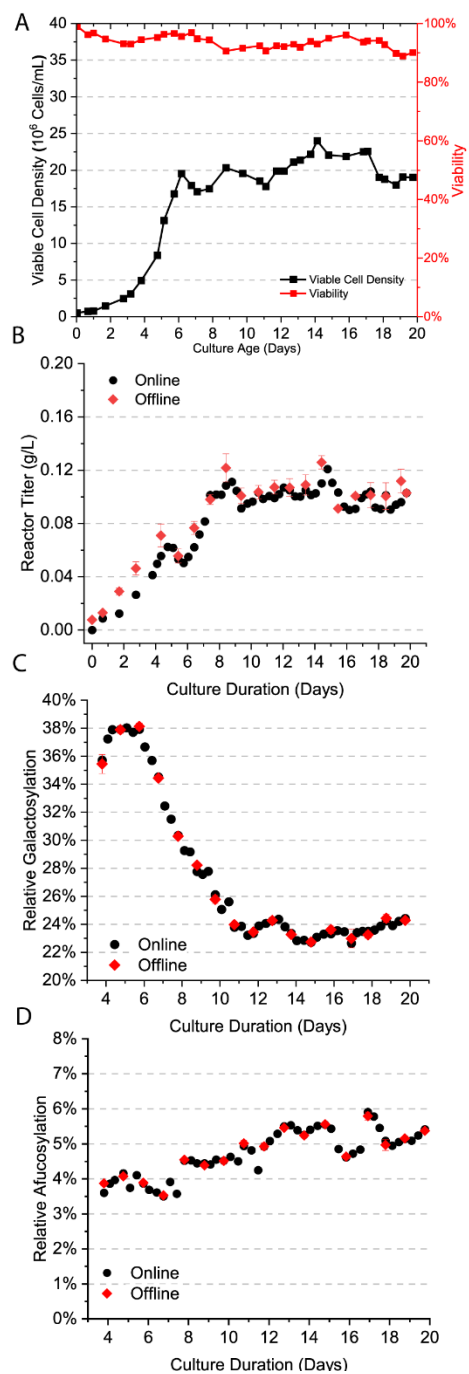
564
565 **Figure 1. Impact on enzymatic deglycosylation reaction time on glycosylamine formation and labeling by IPC:**
566 Monoclonal antibody (~1 g/L) is buffer exchanged into HEPES solution at either pH 7.5 or pH 8.0 and then
567 deglycosylated with PNGase F for varying incubation times from 5 minutes to upwards of 120 minutes (2 hours).
568 Deglycosylated mAbs are all subjected to labeling with IPC immediately after their incubation times, cleaned
569 offline, and then analyzed by HPLC-FLD. **(1A)** Representative chromatograms for the pH 7.5 reaction conditions
570 showing changes in fluorescent intensity over reaction time is shown. **(1B)** Integration of the G0F glycoform to
571 show changes in integrated fluorescence intensity between the two pH conditions over time showing an increase
572 in the amount of labeled glycosylamine at the higher pH condition. All samples were run in $n \leq 3$ replicates.
573



574
575
576
577
578
579
580
581
582
583
584
585

Figure 2. IPC labeled glycan sample cleanup using trap enables efficient labeled glycan separation on analytical column and detection using fluorescence and mass spectrometric detection methods: Increasing injection volumes of IPC labeled N-glycan sample does not cause bias towards relative trastuzumab glycoform abundances at lower injection volumes (ideally < 16 μ l) onto the trap column. (2A) shows the injection and washing of different volumes of samples within a 250 μ l matrix containing 80% acetonitrile and 20% water with no significant variation in residence time on column. (2B) Injection volumes for the three major glycoforms from the trastuzumab biosimilar, while Table 1 shows all glycoforms in tabulated form. (2C) The internal movement of external valve from “sample loading” valve position (1-6) to “HPLC analysis” valve position (1-2). The green lines represent the flow path taken by the sample during specific preparation and analysis steps. (2D) Example HPLC-FLD chromatogram of eluting glycoforms that were also confirmed using an offline LC-MS to indicate the specific mono-isotopic masses detected for each eluting glycan peak.

586



587
588
589
590
591
592
593
594

Figure 3. Online (in black) versus offline (in red) analysis of continuous perfusion bioreactor for mAb titer and major glycan indices are shown here. (3A) Viable cell density and viability over cell culture. (3B) Reactor mAb titer, (3C) Relative mAb galactosylation, and (3D) Relative mAb afucosylation for trastuzumab. Here, online analysis was done using the integrated N-GLYcanizer PAT system employing the IPC workflow, while offline analysis was done using standard offline methods.

595
596 Tables:
597

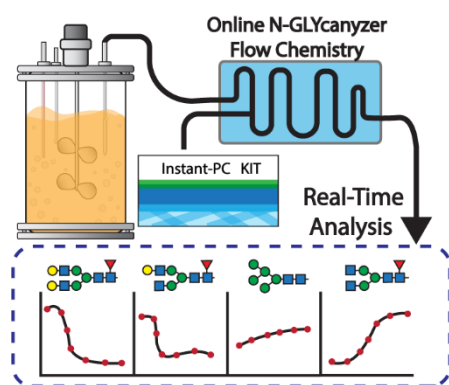
1A	Glycan	Injection size (μL) (AVG+STD) n=2					
		1	2	4	8	16	32
Integrated FLR Value	G0F-GN	0.54 \pm 0.02	0.95 \pm 0.04	1.22 \pm 0.01	2.41 \pm 0.02	4.79 \pm 0.02	5.76 \pm 0.50
	G0	2.84 \pm 0.05	4.62 \pm 0.06	8.39 \pm 0.03	15.96 \pm 0.08	28.01 \pm 1.27	32.57 \pm 0.74
	G0F	35.57 \pm 0.16	57.16 \pm 0.06	117.53 \pm 0.67	229.92 \pm 0.15	378.44 \pm 3.63	484.24 \pm 2.26
	Man5	2.24 \pm 0.06	3.53 \pm 0.14	7.22 \pm 0.10	14.44 \pm 0.25	23.10 \pm 0.28	29.83 \pm 0.26
	G1	0.91 \pm 0.03	1.34 \pm 0.06	2.85 \pm 0.08	5.47 \pm 0.20	8.39 \pm 0.07	11.96 \pm 0.13
	G1F	20.50 \pm 0.06	33.01 \pm 0.13	66.94 \pm 0.16	129.97 \pm 0.12	213.37 \pm 0.98	364.11 \pm 7.14
	G1F'	7.51 \pm 0.03	11.53 \pm 0.13	22.94 \pm 0.11	45.98 \pm 0.11	76.75 \pm 0.48	132.56 \pm 0.83
	G2F	4.21 \pm 0.03	6.46 \pm 0.09	13.29 \pm 0.04	26.77 \pm 0.33	42.77 \pm 0.40	75.00 \pm 1.50

1B	Glycan	Injection size (μL) (AVG+STD) n=2					
		1	2	4	8	16	32
Relative Abundance	G0F-GN	0.7% \pm 0.0%	0.8% \pm 0.0%	0.5% \pm 0.0%	0.5% \pm 0.0%	0.6% \pm 0.0%	0.5% \pm 0.0%
	G0	3.8% \pm 0.0%	3.9% \pm 0.1%	3.5% \pm 0.0%	3.4% \pm 0.0%	3.6% \pm 0.1%	2.9% \pm 0.0%
	G0F	47.9% \pm 0.0%	48.2% \pm 0.1%	48.9% \pm 0.1%	48.8% \pm 0.1%	48.8% \pm 0.1%	42.6% \pm 0.2%
	Man5	3.0% \pm 0.1%	3.0% \pm 0.1%	3.0% \pm 0.1%	3.1% \pm 0.0%	3.0% \pm 0.1%	2.6% \pm 0.0%
	G1	1.2% \pm 0.0%	1.1% \pm 0.1%	1.2% \pm 0.0%	1.2% \pm 0.0%	1.1% \pm 0.0%	1.1% \pm 0.0%
	G1F	27.6% \pm 0.0%	27.8% \pm 0.1%	27.8% \pm 0.0%	27.6% \pm 0.0%	27.5% \pm 0.1%	32.1% \pm 0.3%
	G1F'	10.1% \pm 0.1%	9.7% \pm 0.1%	9.5% \pm 0.0%	9.8% \pm 0.0%	9.9% \pm 0.0%	11.7% \pm 0.2%
	G2F	5.7% \pm 0.1%	5.4% \pm 0.1%	5.5% \pm 0.0%	5.7% \pm 0.1%	5.5% \pm 0.0%	6.6% \pm 0.1%

598
599
600 **Table 1. Relative abundance of IPC-labeled trastuzumab glycoforms during sample recovery from trap column**
601 **cleanup prior to analytical column injection. (1A) Absolute integrated peak fluorescent intensity, and (1B) relative**
602 **absolute abundances of glycoforms from trastuzumab biosimilar at different injection volumes diluted into 250 μL**
603 **80% acetonitrile prepared for injection on trap column. All reported mean values are calculated with at least 2**
604 **technical replicates ($n \leq 2$). The standard deviations are also shown here.**

605
606

607 **Graphical Abstract:**
608



609
610
611
612